Sun Determination of the DustBUSTER CubeSat

Alex St. Clair, Charlie LaBonde, Christine Reilly, Edward Zuzula, Gabe Castillo, Jeff Jenkins, Leina Hutchinson, Rachel Tyler, Reidar Larsen, Robert Hakulin, Ryan Aronson
University of Colorado, Boulder, CO, 80303

With CubeSats emerging as the future of space science, smaller and cheaper systems must be developed to aid in the development and exploration of space. Currently existing sun determination platforms cost thousands of dollars and will not fit inside small CubeSat structures. To combat this issue, a new technique has been developed to use Commercial Off The Shelf (COTS) electrical components, Least Squares Approximations, and QR factorization to provide a sun vector across a 2π steridian view with an accuracy of 1°. This system will fit in a 6U CubeSat frame for the Dust BUSTER (Boulder Unmanned Sensor for Transport Events and Repositioner) project and will compose a significant portion of the Autonomous Re-positioning System (ARS) subsystem.

Nomenclature

$\hat{n}$	=	photodiode normal vector
α	=	angle between photodiode normal vector and Sun vector
X	=	x coordinate of plane intersection
Y	=	y coordinate of plane intersection
Z	=	z coordinate of plane intersection
X_0	=	x coordinate of photodiode normal plane origin
Y_0	=	y coordinate of photodiode normal plane origin
Z_0	=	z coordinate of photodiode normal plane origin
$\vec{X}$	=	least squares solution to matrix system

I. Introduction

Researchers at the Institute for Modeling Plasma, Atmospheric, and Cosmic Dust (IMPACT) have been studying the mechanics of "dust transport events." These dust transport events are characterized by micron size dust particles that exist on the surface of a small celestial body, such as an asteroid or the Moon, and become charged from the solar wind. Once charged, these dust particles are able to be lifted by their coulomb force and appear to jump off the body before returning to the surface. Researchers need data on the charge, mass, and velocity of the charged dust particles to better understand the phenomenon of transport events. While Dust BUSTER will be building a dust instrument to characterize dust transport events, the focus of this paper will be on the sun determination components of the Autonomous Repositioning System (ARS) that is designed to assist the instrument in capturing the events.

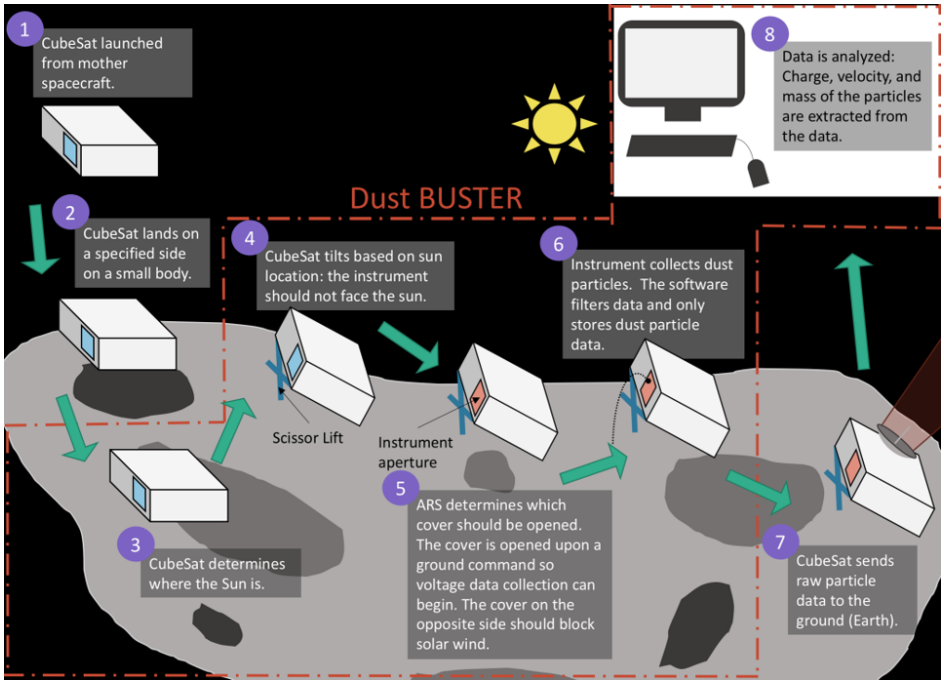

Fig. 1 Dust BUSTER Concept of Operations

The 6U CubeSat will first be ejected by a larger mother spacecraft in orbit around the celestial body. The CubeSat will then descend to the surface and land in a designated orientation. This orientation is controlled by an external mechanism and is not within the scope of the project. In order to detect the charge signals from dust events, the dust instrument must be pointed away from the sun while taking data, avoiding contamination from the solar wind. To address this requirements, as shown in step 3 of Fig. 1, the Autonomous Repositioning System will determine the position of the sun using 13 photodiodes positioned around the CubeSat. The design of the components and determination algorithms are addressed in later sections.

The CubeSat will tilt up to 45° using a scissor lift mechanism and open the dust instrument cover to allow dust particles to fall into the instrument. Using the information about the location of the sun, the CubeSat will determine the maximum acceptable tilt that will keep the instrument free of the solar wind. The collected dust data will then be sent to either the mother spacecraft, or in the case of the project, to an external computer for processing.

II. Design Objectives

To aid in the characterization of the dust transport events, the ARS is designed with the following objectives in mind:

1) The ARS shall determine where the Sun is located relative to the instrument apertures.
2) The ARS shall have sensors to collect data about the position of the Sun.
3) The ARS shall determine Sun position to within ± 5° up to 45° above the surface and to within ±1° from 45° to 90° above the surface.
4) The ARS shall determine the angular region in which an instrument opening will be fully shaded, using the determined Sun vecotor.
5) The ARS shall maintain full view of the sky in a 180 degree half dome over the +Z hemisphere, determined by the CubeSat's original resting position.

III. Photodiode Design

A. Design Overview

To achieve the above objectives, the design shown in Fig. 2 is used.

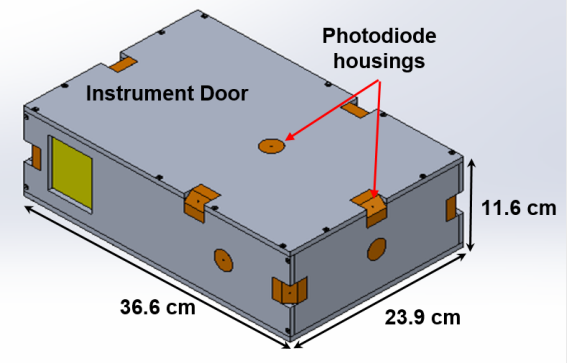

Fig. 2 CubeSat model

The photodiode covers are shown in orange placed around the CubeSat. There are 13 photodiodes placed on the faces and vertices of the CubeSat. This allows the system to determine the position of the Sun at all points in the sky. The unique design of the photodiode aperture, shown in Fig. 3, allows the photodiode to sense changes in the light intensity as a function of incidence angle. The photodiodes are allowed a field of view of 60 degrees.

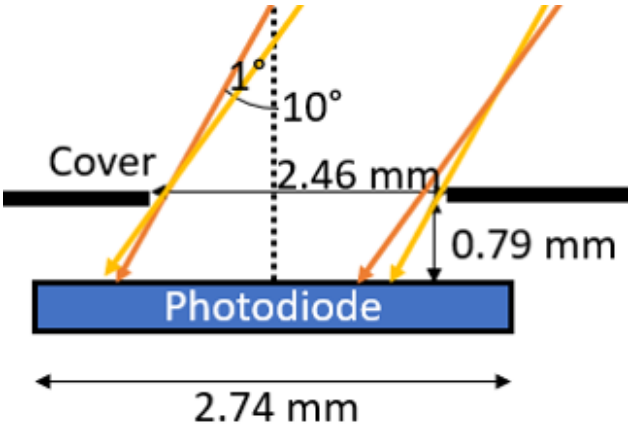

Fig. 3 Photodiode Cover Design

As the incidence angle increases, the output of the photodiode decreases. This allows us to determine the angle between the Sun and the boresight of the photodiode. The cover itself, shown in Fig. 4, allows the printed circuit board (PCB), shown in grey, to remain firmly up against the cover aperture while mounted to the CubeSat structure. The photodiode itself is mounted on the PCB.

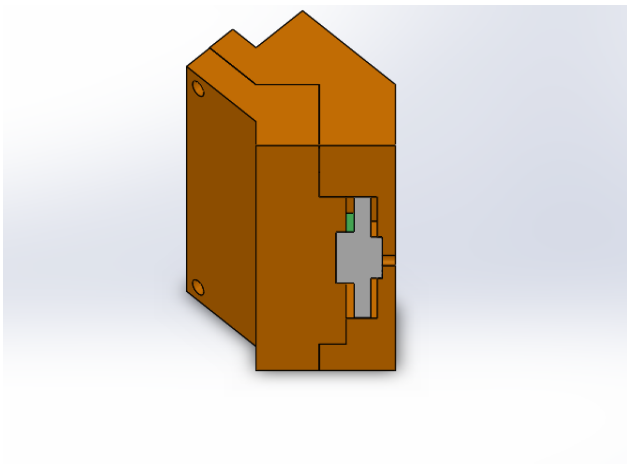

Fig. 4 Photodiode Cover Cut Away View

B. Numerical Results

To begin validation of this design, several numerical experiments were conducted to verify that the physical system would be able to satisfy the full sky coverage requirement. In particular, the Sun must always be within the field of view of 3 separate photodiodes so that the 3-dimensional Sun vector can be reconstructed. For testing, the full sky was discretized by 1 degree increments in both azimuth and elevation angles, creating a grid of points used as the possible Sun locations. With the Sun at each of these locations, the angle between the Sun vector and each photodiode was computed, and if this angle was less than the 60 degree allowed field of view the photodiode was able to "see" the Sun. The results of this experiment are shown in Fig. 5, where the shading represents the number of photodiodes able to see the Sun in the location given by the elevation angle (y-axis) and azimuth angle (x-axis). Clearly there were no locations in the sky where the Sun would be seen by fewer than 3 photodiodes, suggesting that the requirement was satisfied.

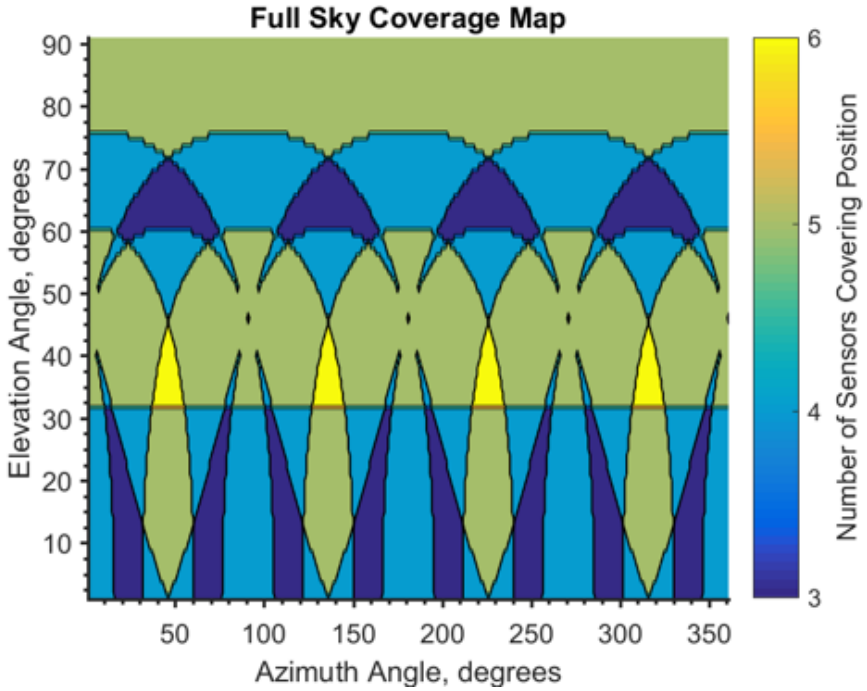

Fig. 5 Number of Photodiodes Over Full Sky

However, this only verified the requirement in the nominal design case. In all likelihood there will be errors during the manufacturing process, and thus the photodiodes will not end up exactly in their nominal positions. To model potential errors, a Monte Carlo analysis was conducted, which uniformly varied the amount of deviation in the angular position of each photodiode. The maximum deviation was tested at 1, 2, 3, 4, 5, and 6 degrees. For each maximum, 1000 random configurations of photodiodes were tested to see if there were any points in the sky not covered. Figure 6 details the results of this study. From this study it is clear that so long as the mounting error remains below 5 degrees we can be fairly sure that the system will be able to achieve full sky coverage. With larger mounting errors a non-negligible number of unsatisfactory configurations of photodiodes arise.

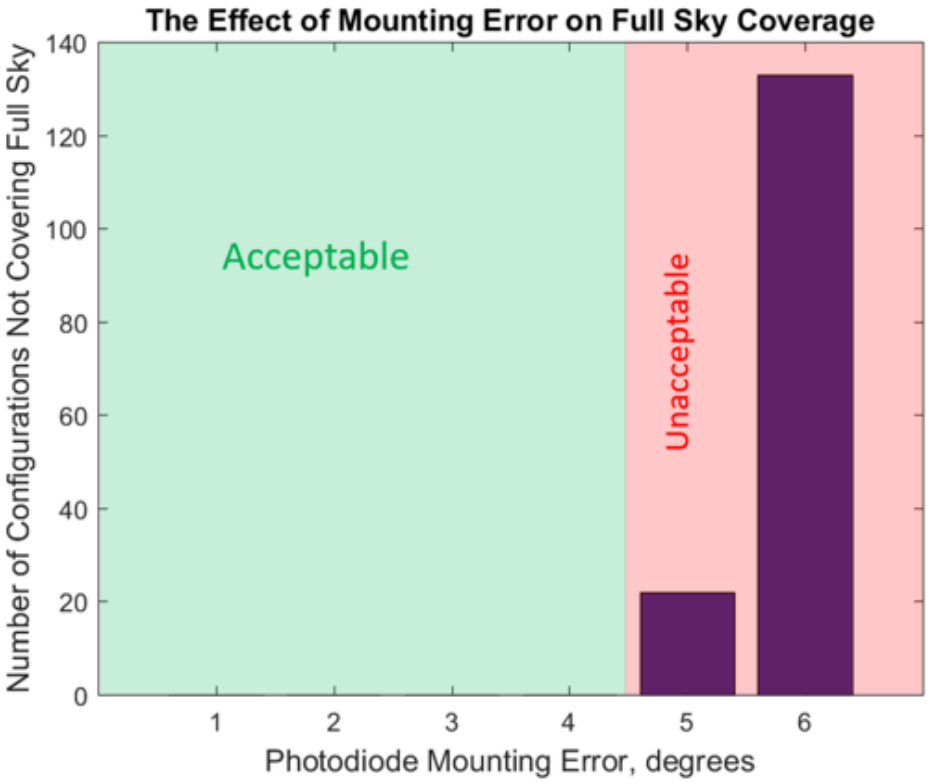

Fig. 6 Full Sky Coverage Dependent on Mounting Errors

IV. Sun Finding Algorithm

A. Theory

Now that the physical sun finding system has been described, we can begin to discuss the mathematical methodology used to locate the sun's position. To begin, various assumptions are made about the physical system. First, we assume for simplicity that there is no error in the mounting locations of the photodiodes. This will not be the case in reality, but the effect of mounting errors will be quantified in the following numerical results section. In addition, the translational offsets of the photodiodes are ignored, meaning that the normal axes of all of the photodiodes intersect at the origin. As the distance from the CubeSat to the Sun is extremely large, this assumption will only results in errors in the Sun vector on the order of 10^{-10} degrees, well within our accuracy requirements.

The first step in the Sun finding algorithm is to define the normal vectors pointing out of each photodiode, shown in Fig. 7. These vectors are determined by the placement of each photodiode, described above. Note that in this figure only 3 photodiode normals are depicted for simplicity, and these vectors are colored red, blue, and green. The sun vector is represented in yellow.

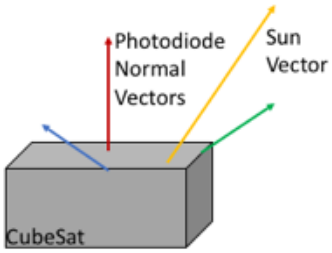

Fig. 7 Initial Setup for Algorithm

Each photodiode will output a voltage corresponding to an angle describing the sun's location relative to the photodiode normal vector. Three photodiodes are selected which have the Sun in their respective 60 degree fields of view. Then, the Sun vector is projected onto each of photodiode normals, which creates parallel and perpendicular components as shown in Fig. 8. If we assume that the Sun vector is of unit length, then the magnitude of the parallel components are simply given by the cosine of the corresponding measured angles. Similarly, the magnitude of the perpendicular component of the Sun vector is given by the sine of the angle.

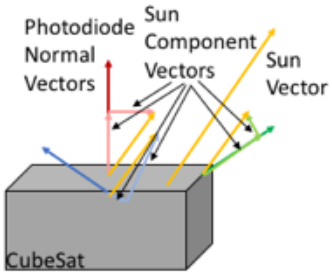

Fig. 8 Sun Vector Components

However, the direction of the perpendicular component of the Sun vector cannot be determined uniquely. In fact, it can lie anywhere in the orthogonal complement of the photodiode normal, which is the plane normal to this vector defined by Eq. 1 below. In this equation the plane's origin is represented component wise as X_0, Y_0, Z_0. The points that lie on the plane are represented as X, Y and Z. The components of the $\hat{n}$ vector are represented as $\hat{n}_x, \hat{n}_y$, and $\hat{n}_z$. If we solve for the unknown sun vector components we arrive at Eq. 2.

$$\begin{aligned} \hat{n}_x(X - X_o) + \hat{n}_y(Y - Y_o) + \hat{n}_z(Z - Z_o) &= 0 \\ \hat{n}_x(X - \hat{n}_x \cos\alpha) + \hat{n}_y(Y - \hat{n}_y \cos\alpha) + \hat{n}_z(Z - \hat{n}_z \cos\alpha) &= 0 \end{aligned} \tag{1}$$

$$\hat{n}_x(X) + \hat{n}_y(Y) + \hat{n}_z(Z) = \hat{n}_x^2 \cos\alpha + \hat{n}_y^2 \cos\alpha + \hat{n}_z^2 \cos\alpha \tag{2}$$

However, as we have one plane created by each of the three photodiodes being considered, we see a situation similar to the one described by Fig. 9. We then obtain 3 equations of the form given by Eq. 2, and we can arrange this into a linear system as shown in Eq. 3, where $\hat{n_{11}}, \hat{n_{12}}$ and $\hat{n_{13}}$ correspond to the X, Y, and Z components of the first photodiode, $\hat{n_{21}}, \hat{n_{22}}$ and $\hat{n_{23}}$ correspond to the X, Y, and Z components of the second photodiode, and $\hat{n_{31}}, \hat{n_{32}}$ and $\hat{n_{33}}$ correspond to the X, Y, and Z components of the third photodiode. The angles of these three photodiodes are different and are represented as α_1, α_2 and α_3,and X, Y and Z represent the intersection of the three planes. Assuming linear independence of the photodiode normal vectors, the three planes must intersect in a single point, shown by the intersection of the dotted lines in Fig. 9. The vector from the origin through this point then defines the direction of the sun vector.

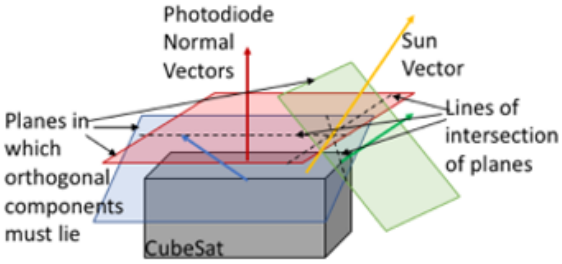

Fig. 9 Three Orthogonal Plane Containing Perpendicular Sun Vector Components

$$\begin{bmatrix} \hat{n}_{11} & \hat{n}_{12} & \hat{n}_{13} \\ \hat{n}_{21} & \hat{n}_{22} & \hat{n}_{23} \\ \hat{n}_{31} & \hat{n}_{32} & \hat{n}_{33} \end{bmatrix} \begin{bmatrix} X \\ Y \\ Z \end{bmatrix} = \begin{bmatrix} \hat{n}_{11}^2 \cos\alpha_1 + \hat{n}_{12}^2 \cos\alpha_1 + \hat{n}_{13}^2 \cos\alpha_1 \\ \hat{n}_{21}^2 \cos\alpha_2 + \hat{n}_{22}^2 \cos\alpha_2 + \hat{n}_{23}^2 \cos\alpha_2 \\ \hat{n}_{31}^2 \cos\alpha_3 + \hat{n}_{32}^2 \cos\alpha_3 + \hat{n}_{33}^2 \cos\alpha_3 \end{bmatrix} \tag{3}$$

Now, up until this point it has been assumed that the sun was only within the field of view of exactly three photodiodes. However, as we showed previously there are many locations at which more than three photodiodes would be in view of the sun. Thus we would like to have a methodology to utilize the measurements from all of the relevant photodiodes in order to improve of the accuracy of the sun location estimate. To do this we apply the least squares methodology. In the case that there are more than three photodiodes that can see the sun, we have the definitions of more than three planes, and thus we have more rows than columns in the left-hand side matrix of Eq. 3. This becomes an overdetermined system which cannot be solved exactly in general, meaning that there will not be one point of intersection between all of the planes. However, by instead solving the normal equations, shown in Eq. 4, we obtain the least-squares solution to the problem, which represents the point closest to an intersection of all planes.

$$(A^T)A\vec{X} = A^T b \tag{4}$$

B. Numerical Results

In order to test this algorithm before committing to the use of actual hardware and flight software, various simulations were conducted using MATLAB. To begin, the mathematically ideal model described in the previous section was considered. The full sky was discretized into discrete points at which the sun was placed to create many different scenarios, and then this algorithm was tasked with determining the sun vector based on simulated photodiode outputs. Then, the angle between the calculated sun vector and the actual sun vector was calculated and defined to be the error associated with the model. For these scenarios the maximum angular error was on the order of 10^{-16} degrees. This is the limit of double precision in MATLAB, revealing that the algorithm was essentially reconstructing an exact sun vector.

Of course, this ideal model is hardly indicative of the actual performance of the algorithm when used with the physical systems. To more accurately simulate actual operation, digital resolution limitation and electrical noise effects were added into the simulated photodiode measurements. The sun was then again placed throughout the full sky and the model determined the sun vector. The resulting errors over the full sky were then compiled into a histogram describing the frequency of those errors, shown in Fig. 10. Clearly all of the errors in the vector calculations were much less than the 1 degree accuracy requirement placed on the sun detection system for the Dust BUSTER project, represented by the red line.

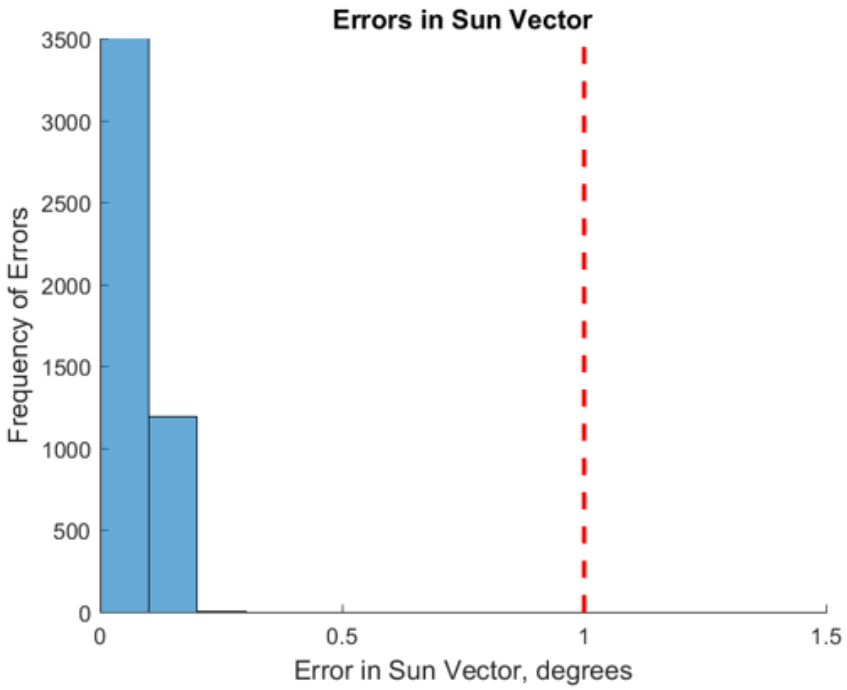

Fig. 10 Errors in Sun vector including resolution and noise effects

However, noise effects will likely not be the largest contributor to the error produced by the algorithm. In addition to noise, effects of errors in the mountings of the photodiodes relative to their nominal design locations were considered. The photodiode normal vectors were randomly perturbed by up to either 1 degree or 0.5 degrees in any direction, and again simulations were run with the sun at a multitude of locations in the sky. Figure 11 details the resulting errors in these simulations. It is clear that in the 1 degree case there were locations at which the error in the calculated sun vector was greater than the accuracy requirement. However, the 0.5 degree case did in fact satisfy the requirements.

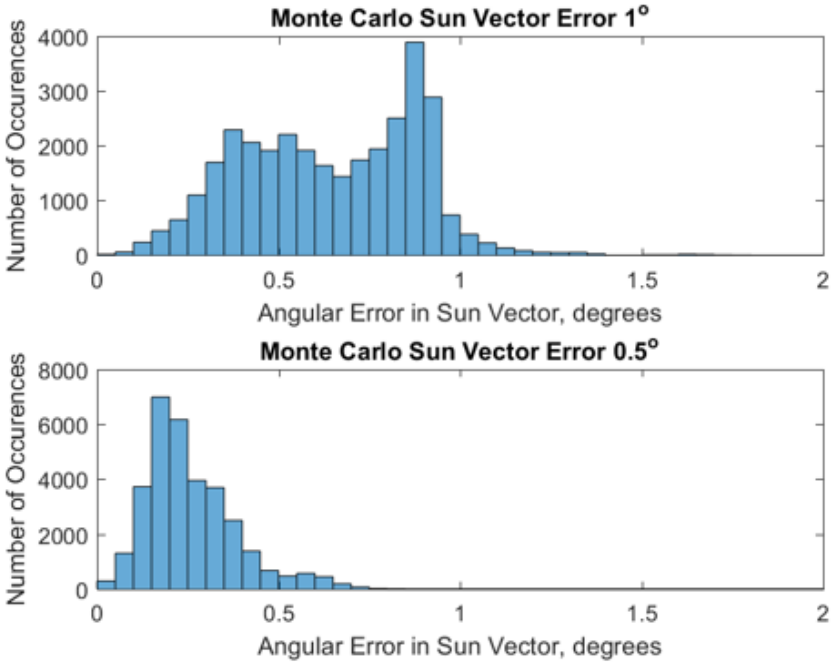

Fig. 11 Errors in Sun vector including photodiode mounting effects

This analysis seemed to suggest that the photodiodes must be mounted to the CubeSat body within 0.5 degrees of the nominal design locations for acceptable performance from the sun determination subsystem. However, this is not exactly the case. This algorithm assumes that the photodiode normal is pointed in exactly the direction defined by the nominal mounting location. If there are mounting errors these calculations quickly become inaccurate as the algorithm has no notion of the actual orientation of the photodiodes, and thus there are larger errors in the Sun vector. However, it was shown above that small variations in mounting do not affect the ability of the system to achieve full sky coverage, which suggests that some degree of mounting error is acceptable. If we then update the algorithm to account for the actual normal directions after mounting, we should obtain more accurate results. Pulling together the results from all of the experiments performed leads to the conclusion that the photodiode normal vector must simply be known to within 0.5 degrees, which is much more feasible than mounting to within 0.5 degrees of the nominal position. Therefore, calibration will be performed with the system once the photodiodes are installed, to determine the actual mounting direction. These results have given confidence that this system will be able to meet all of the relevant design requirements.

V. Conclusion

This paper described a system for making accurate sun location measurements using COTS components in the context of the DustBUSTER CubeSat mission being designed by the Dust BUSTER senior projects team at the University of Colorado Boulder. A design which offered full sky coverage using an array of photodiodes was detailed, through numerical simulations evidence was provided that the system would satisfy the design requirements of the mission.

Once testing has been completed the effectiveness of the system will be addressed.

Acknowledgments

The Dust BUSTER team would like to acknowledge Professor Torin Clark for his advisory role in this project. In addition the team would like to thank the rest of the Project Advisory Board at the University of Colorado Boulder for their design help and feedback.

References

[1] Wang, X., J. Schwan, H.-W. Hsu, E. Grün, and M. Horányi (2016), Dust charging and transport on airless planetary bodies, Geophys. Res. Lett., 43, 6103–6110, doi:10.1002/2016GL069491.

[2] Duncan, N., Z. Sternovsky, E. Grün, S. Auer, M. Horanyi, K. Drake, J. Xie, G. Lawrence, D. Hansen, and H. Lee (2011), The Electrostatic Lunar Dust Analyzer (ELDA) for the detection and trajectory measurement of slow-moving dust particles from the lunar surface, Planetary and Space Science, 59, 1446-1454, doi:10.1016/j.pss.2011.06.002.